Supplement of Atmos. Chem. Phys., 20, 3999–4011, 2020
https://doi.org/10.5194/acp-20-3999-2020-supplement
© Author(s) 2020. This work is distributed under
the Creative Commons Attribution 4.0 License.

Supplement of

Heterogeneous formation of particulate nitrate under ammonium-rich regimes during the high-$PM_{2.5}$ events in Nanjing, China

Yu-Chi Lin et al.

Correspondence to: Yan-Lin Zhang (dryanlinzhang@outlook.com, zhangyanlin@nuist.edu.cn)

The copyright of individual parts of the supplement might differ from the CC BY 4.0 License.

Contents of this file

There are two sections, one table and seven figures in the supporting materials. Supplementary Sec. 1 describes the equations in calculation of theoretical equilibrium constant between gaseous HNO_3 and NH_3 and particulate NH_4NO_3 under specific ambient T and RH conditions. Supplementary Sec. 2 describes the equation to estimate the production rate of nitrate aerosols during the high-$PM_{2.5}$ events.

Supplementary Sec. 1

The reaction of $HNO_3 + NH_3$ is an important pathway to produce particulate NH_4NO_3. In the equilibrium of $HNO_{3(g)} + NH_{3(g)} \rightarrow NH_4NO_{3(s,\ aq)}$, the theoretical equilibrium constant between gaseous HNO_3 and NH_3, and particle NH_4NO_3 (k_2 of R2 in the main text) can be calculated as (Mozurkewich, 1993):

$$\ln(k_2) = 118.87 - \frac{24084}{T} - 6.025\ln(T) \tag{S1}$$

where T is ambient temperature with a unit of °K. As the ambient RH (aw=RH/100) is higher than the deliquescence relative humidity of NH_4NO_3 (DRH, approximately 62 % RH at atmospheric standard condition), the influence of ambient RH on k_2 should be considered. Thus, k_2 should be replaced by k_2', namely:

$$k_2' = (P_1 - P_2(1-a_w) + P_3(1\text{-}a_w)^2) \times (1\text{-}a_w) \times (1\text{-}a_w)^{1.75} \times k_2 \tag{S2}$$

where

$$\ln(P_1) = -135.94 + \frac{8763}{T} + 19.12\ln(T) \tag{S3}$$

$$\ln(P_2) = -122.65 + \frac{9969}{T} + 16.22\ln(T) \tag{S4}$$

$$\ln(P_3) = -182.61 + \frac{13875}{T} + 24.46\ln(T) \tag{S5}$$

Using an appropriate expression for the T and RH dependence of NH_4NO_3 thermodynamic properties, the equilibrium constant can be calculated at a specific temperature and relative humidity.

Supplementary Sec. 2

In Table S1, we defined the $PM_{2.5}$ haze days with hourly $PM_{2.5}$ concentrations of exceeding 150 μg m^{-3} and the high $PM_{2.5}$ levels should be lasted more than 3 hours. During the high $PM_{2.5}$ events, the maximum production rate of absolute nitrate concentrations (AF_{NO3-}, μg m^{-3} h^{-1}) can be calculated as:

$$AF_{NO_3^-} = \frac{([NO_3^-]_m - [NO_3^-]_i)}{([CO]_m / [CO]_i)\Delta h} \tag{S6}$$

where $[NO_3^-]_i$ is the nitrate concentration at the initial time during the $PM_{2.5}$ event. $[NO_3^-]_m$ is the maximum nitrate concentrations during the $PM_{2.5}$ event. Both parameters are in units of μg m^{-3}. Δh (hours) denotes the duration time between the initial time and the time when NO_3^- concentration reached to the maximum value during the $PM_{2.5}$ event. $[CO]_m$ is the CO concentration when the NO_3^- concentration reached to the maximum value during the $PM_{2.5}$ event. $[CO]_i$ is the CO concentration at the initial time during the $PM_{2.5}$ event. Both units of $[CO]_m$ and $[CO]_i$ are in units of ppm. Here, $[CO]_m/[CO]_i$ can be considered a dilution factor of the atmosphere. Furthermore, the relative production rate of nitrate (RF_{NO3-}, % h^{-1}) can be calculated as:

$$RF_{NO_3^-} = \frac{([NO_3^-]_m - [NO_3^-]i)}{([CO]_m / [CO]_i)\Delta h [NO_3^-]_i} \tag{S7}$$

Table S1 Summarized information for occurrence of high $PM_{2.5}$ events, formation rate and potential mechanisms for particulate NO_3^-.

Events	Time of occurrence	Production rate of NO_3^- (% h^{-1})[a]	Behaviors of AWLC and Ox	Potential mechanisms
2016				
Case I	3/3 18:00 – 3/4 03:00	5.5 (2.3)	ALWC and Ox Kept constant levels	$NO_2 + OH$ / $N_2O_5 + H_2O$
Case II	3/4 07:00 – 3/4 15:00	2.4 (1.0)	Decreasing ALWC and increasing Ox	$NO_2 + OH$
Case III	3/4 23:00 – 3/5 03:00	26.7 (11.4)	Increasing ALWC and decreasing Ox	$N_2O_5 + H_2O$
Case IV	3/5 14:00 – 3/5 21:00	15.4 (5.0)	Increasing ALWC and decreasing Ox	$N_2O_5 + H_2O$
Case V	3/6 09:00 – 3/6 20:00	2.5 (0.6)	Decreasing ALWC and increasing Ox	$NO_2 + OH$
Case VI	3/14 22:00 – 3/15 04:00	6.0 (2.6)	Increasing ALWC and increasing Ox	$NO_2 + OH$ / $N_2O_5 + H_2O$
Case VII	3/18 09:00-3/18 18:00	13.7 (5.2)	Increasing ALWC and decreasing Ox	$N_2O_5 + H_2O$
Case VIII	3/19 07:00 – 3/19 16:00	11.0 (2.5)	Decreasing ALWC and decreasing Ox	$NO_2 + OH$ / $N_2O_5 + H_2O$
Case IX	5/7 02:00 – 5/7 08:00	4.0 (0.8)	Increasing ALWC and decreasing Ox	$N_2O_5 + H_2O$
2017				
Case X	1/23 17:00 -1/23 21:00	10.4 (1.0)	Increasing ALWC and Ox kept constant levels	$N_2O_5 + H_2O$
Case XI	2/6 00:00 – 2/6 05:00	11.4 (3.5)	Increasing ALWC and Ox kept constant levels	$N_2O_5 + H_2O$
Case XII	2/13 22:00 – 2/14 06:00	6.7 (1.8)	Increasing ALWC and Ox kept constant levels	$N_2O_5 + H_2O$

[a] The values in the parentheses are the production rates of NO_3^- in units of μg m^{-3} h^{-1}.

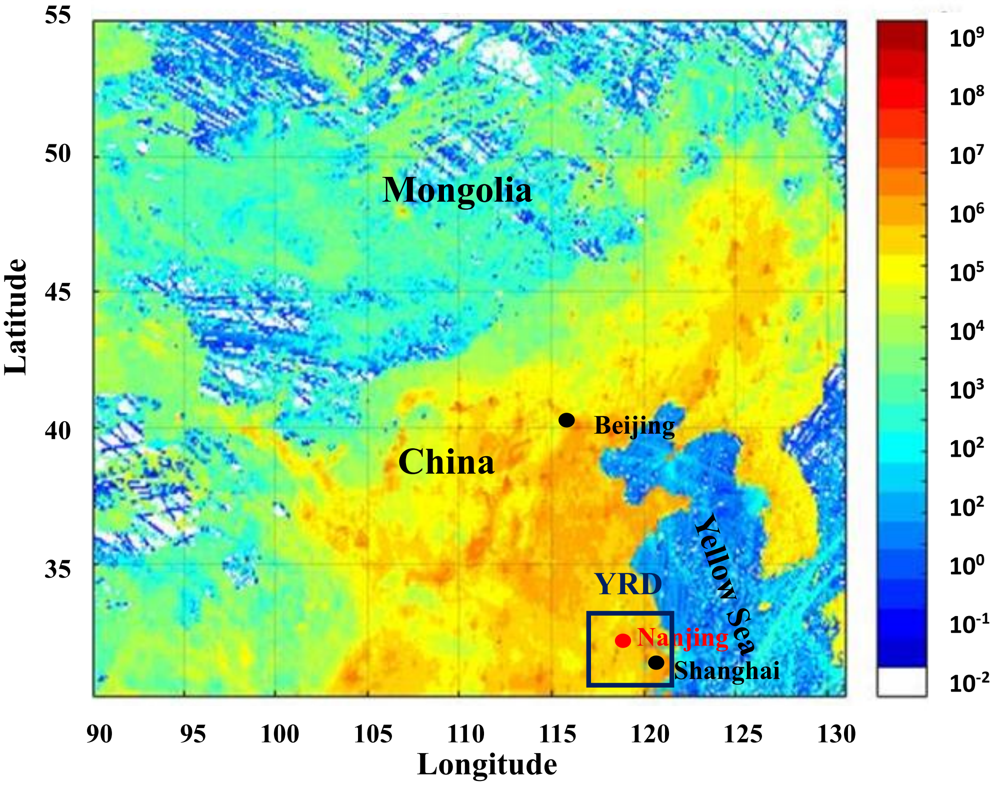

Figure S1 Relative locations of the sampling site**.** In this figure, the sampling site (Nanjing) is marked by the red dot. The contour denotes $PM_{2.5}$ emission data (kg km^{-1} $month^{-1}$), which is obtained from Huang et al. (2014b).

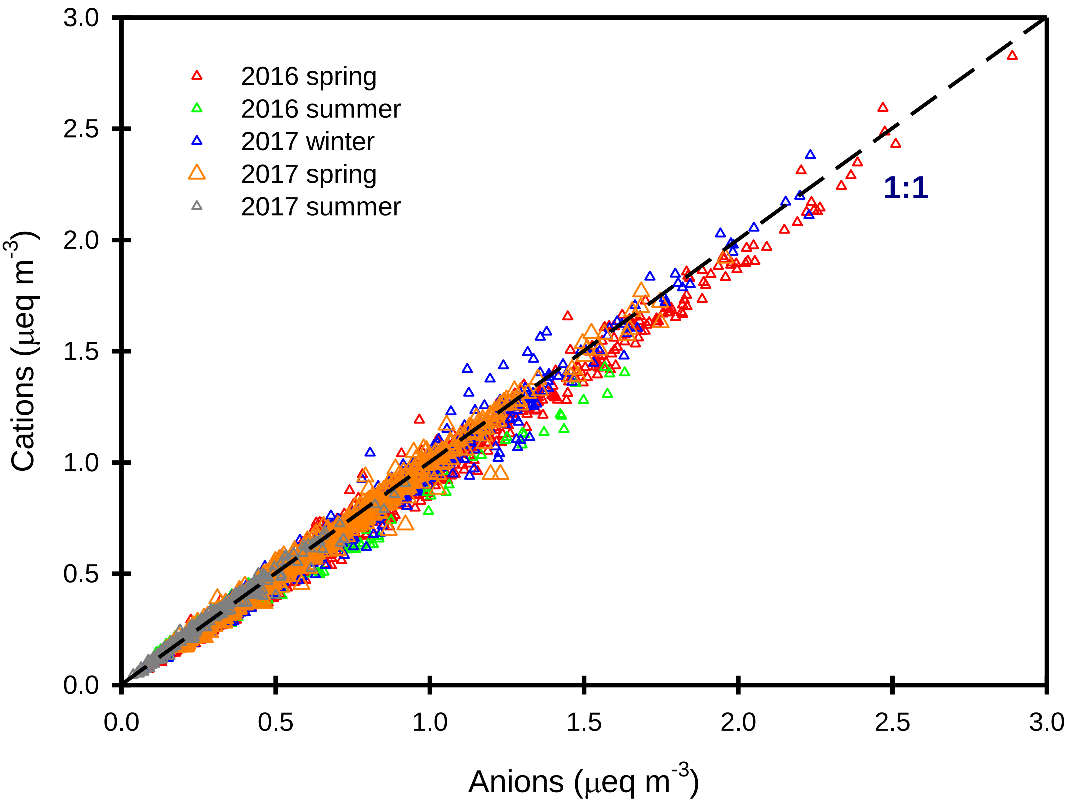

Figure S2 Equivalent concentrations of cations and anions in $PM_{2.5}$ in Nanjing during the sampling periods.

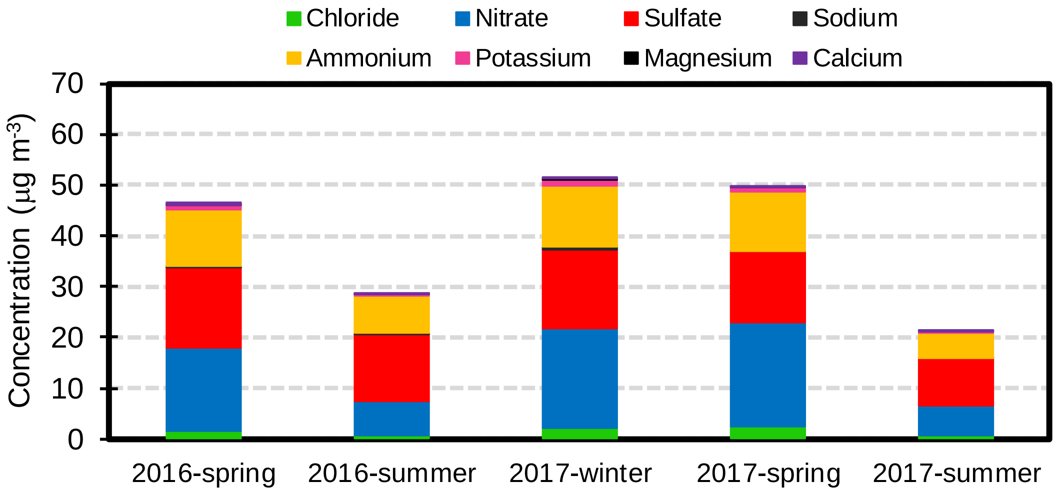

Figure S3 Average concentrations of water-soluble inorganic ions in $PM_{2.5}$ observed in Nanjing during the different seasons.

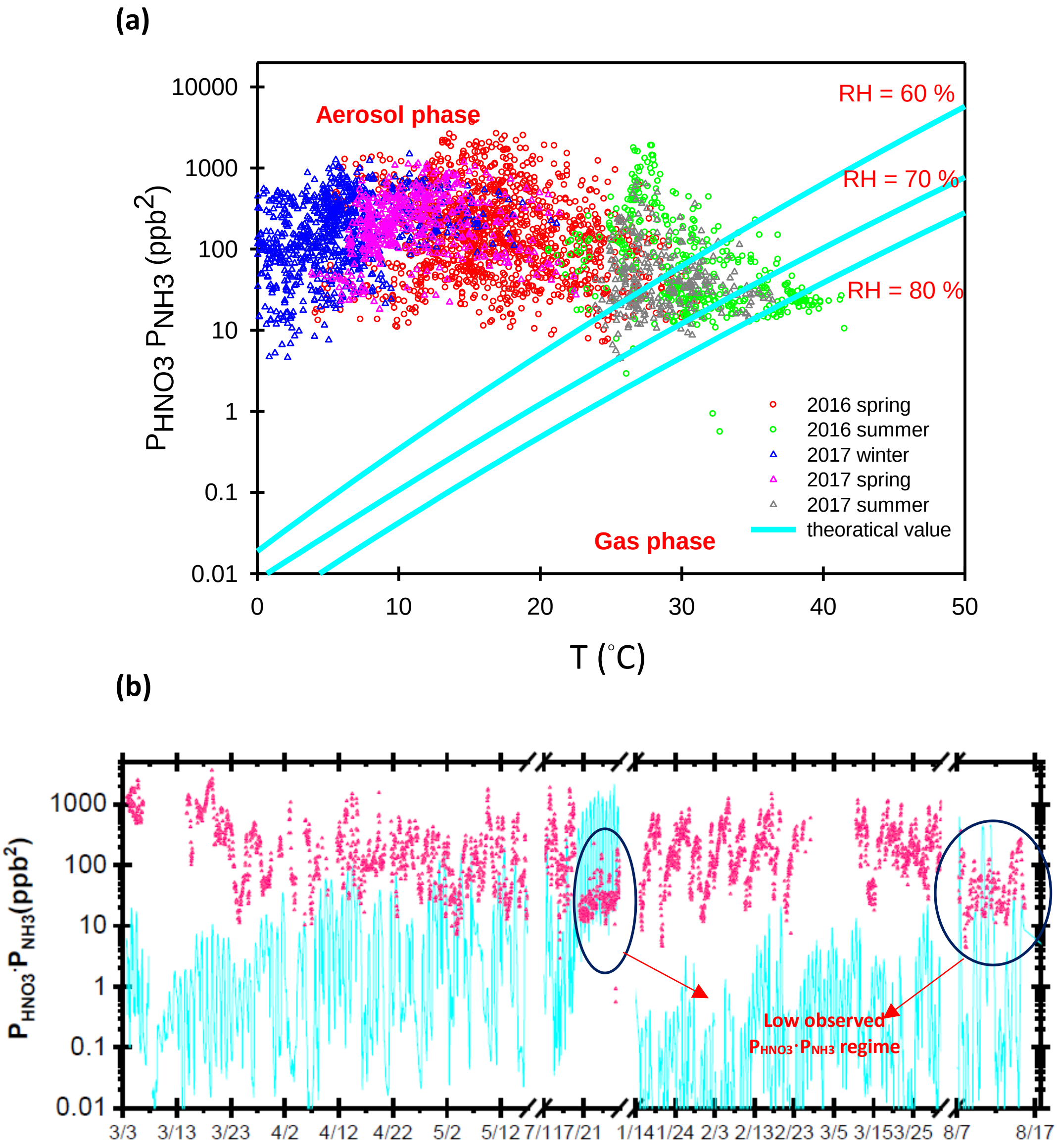

Figure S4 (a)Theoretical (solid lines) and observed (circles and triangles) equilibrium constants of partitioned NO_3^- and NH_4^+ between aerosol and gas phase in different ambient temperature and relative humidity, and (b) time series of theoretical (blue line) and observed equilibrium constants (pink dots) during the sampling periods. The observed equilibrium constants are the products of observed total nitrate (TN, TN=NO_3- + HNO_3) and total ammonium (TA, TA=NH_4^+ + HN_3).

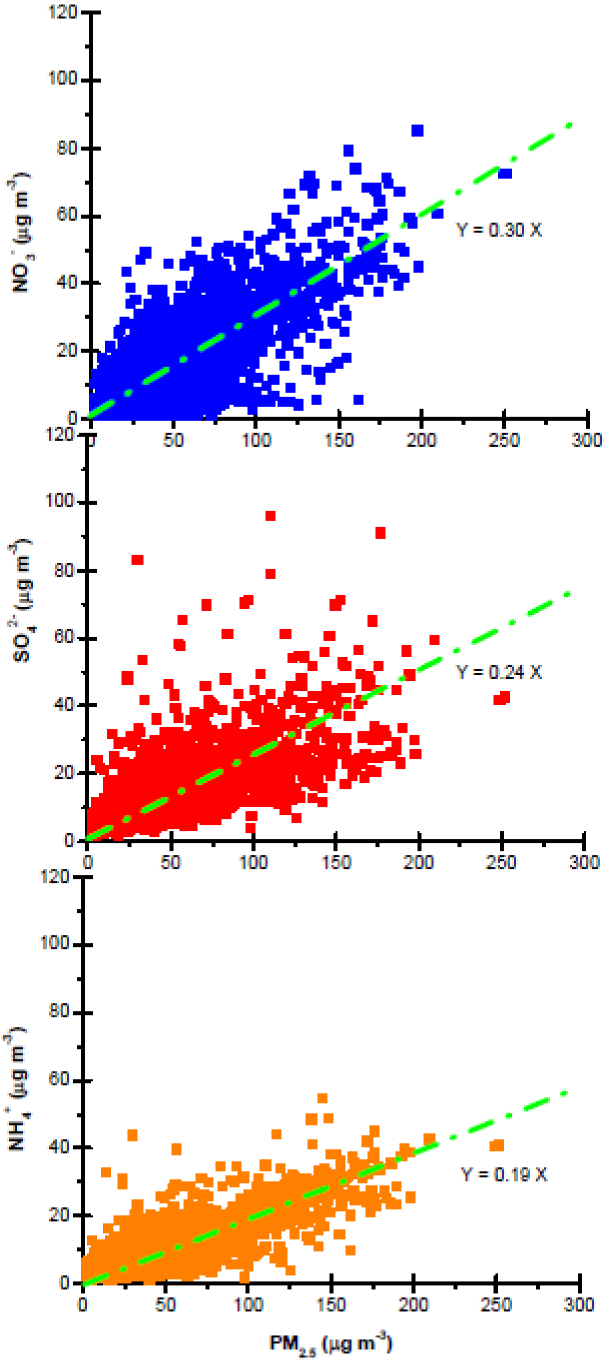

Figure S5 Scatter plots of NO_3^-, SO_4^{2-} and NH_4^+ against $PM_{2.5}$ mass in Nanjing during the sampling periods.

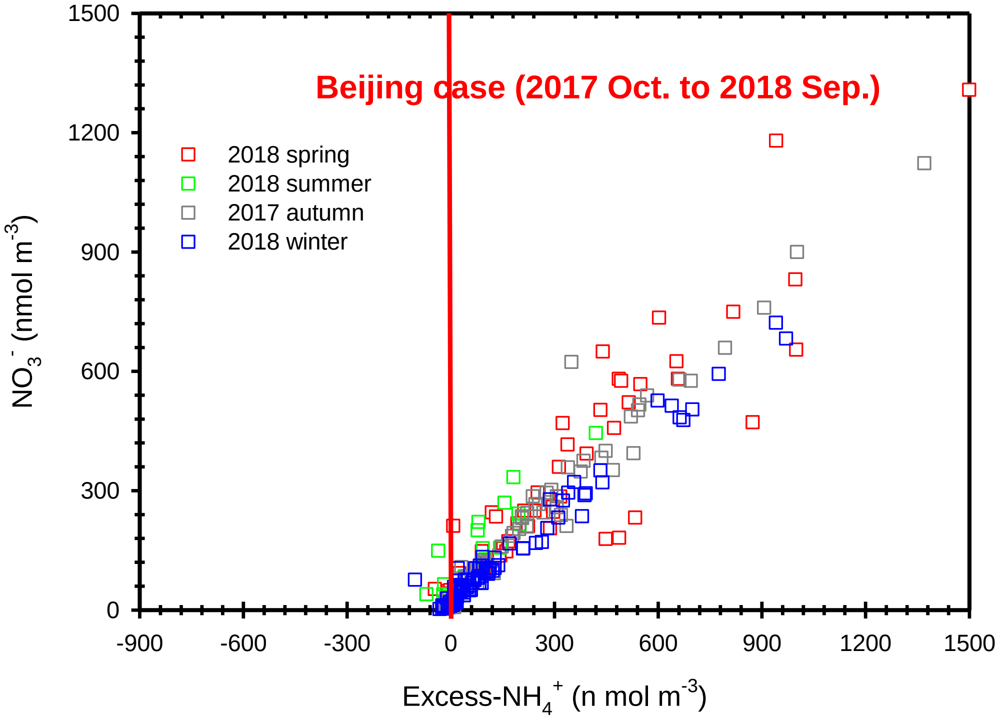

Figure S6 Scatter plots of NO$_3^-$ vs. excess-NH$_4^+$ molar concentrations in Beijing from October 2017 to September 2018. The data is obtained from Dao et al. (2019).

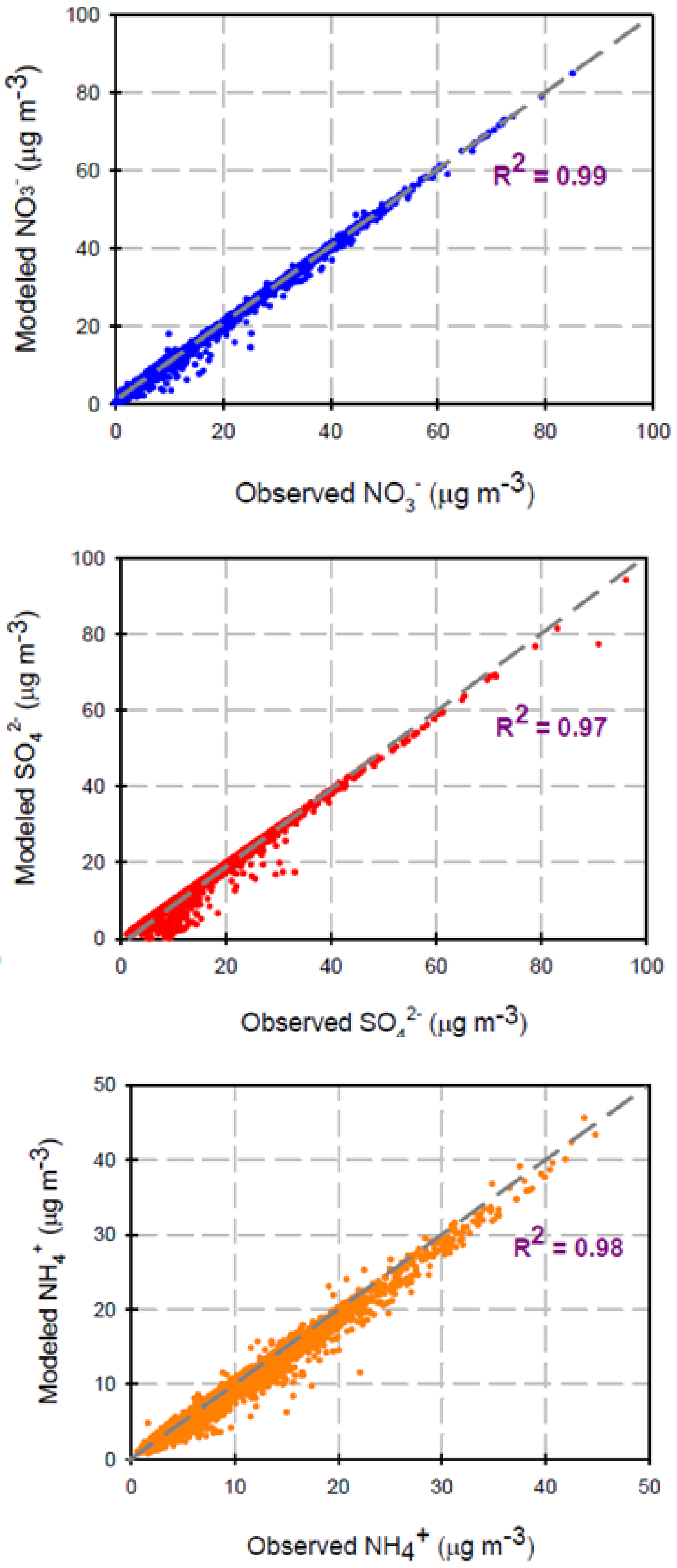

Figure S7 Scatter plots of modeled results vs. observations of NO_3^-, SO_4^{2-} and NH_4^+ in $PM_{2.5}$ in Nanjing during the sampling periods.

References

Dao, X., Lin, Y.-C., Cao, F., Di, S.-Y., Hong, Y., Xing, G., Li, J., Fu, P., and Zhang, Y.-L. Introduction to the aerosol chemical composition monitoring network of China: objects, current status and outlook. *B. AM. Meteorol. Soc.*, 100, ES337-ES351, https://doi.org/10.1175/BAMS-D-18-0325.1, 2020.

Huang, Y., Shen, H., Chen, H., Wang, R., Zhang, Y., Su, S., Chen, Y., Lin, N., Zhong, Q., Wang, X., Liu, J., Li, B., Liu, W., and Tao, S.: Quantification of global primary emissions of $PM_{2.5}$, PM_{10} and TSP from combustion and industrial process sources. *Environ. Sci. Technol.,* 48, 13834-13843, https://doi.org/10.1021/es503696k, 2014.

Mozurkewich, M.: The dissociation constant of ammonium nitrate and its dependence on temperature, relative humidity and particle size. *Atmos. Environ.,* 27, 261-270, https://doi.org/10.1016/0960-1686(93)90356-4, 1993.